

# X Ray Photon Correlation Spectroscopy for the Study of Polymer Dynamics.

---

*Aurora Nogales<sup>1</sup> and Andrei Flueraș<sup>2</sup>*

*<sup>1</sup> Instituto de Estructura de la Materia, IEM-CSIC.*

*<sup>2</sup> Brookhaven National Laboratory, NSLS-II, Upton, NY 11973*

## Abstract

X Ray Photon Correlation Spectroscopy, XPCS, is a novel technique developed for the study of slow dynamics in condensed matter. The principle of this technique is based on the time variations of the speckle pattern originated by the scattering of coherent light from a material with spatial inhomogeneities. Although laser photon correlation spectroscopy was long established, XPCS has only been possible with the advent of new synchrotron radiation X-ray sources that can provide sufficient coherent flux. The results from these techniques and future perspectives in the field of polymer science are discussed here.

The macroscopic properties of polymer materials are determined by the interplay between different processes that occur in a wide range of time and length scales. From a structural viewpoint, polymer materials are complex. The constituent repeating units, i.e., the monomers lay in the nanometer range, whereas the size of a whole polymer chain, characterized by its radius of gyration ( $R_g$ ) might be around several tenths of nanometers. Besides, polymer chains in bulk are typically coiled and entangled with each other forming a network. This structural hierarchy is also accompanied by a very wealthy dynamics ranging from fast processes like bond vibrations, in the picosecond regime, passing on the segmental dynamics range, in the millisecond range, to the flow of the polymer melt with characteristics times that may achieve the seconds range.

This broad range dynamics has been traditionally explored by a combination of methods. Among them, one can distinguish between those that explore the dynamics macroscopically, without considering the length scale of the motion, and those that provide also spatial information related to the dynamic process. Examples of the first class are infrared and Raman spectroscopies that study bond vibrations [1, 2], or broadband dielectric spectroscopy that allows the investigation of slower processes, like the alpha relaxation associated to the glass transition [3]. Among the methods that provide space/time resolution at relevant scales for polymer dynamics, neutron scattering techniques have been the most used, since besides the spatial resolution, deuterium labelling adds selectivity and allows to study motions of particular groups or segments from complex polymer

materials [4]. The study of polymer dynamics by light scattering techniques, although in principle tempting, has had more limited applications because of several reasons, as discussed below. Of particular interests are techniques such as light photon correlation spectroscopy (LPCS) which enable direct measurements of the dynamic structure by using time correlation functions [5] of the (fluctuating) scattered intensity. LPCS measures the dynamic structure factor over a wide temporal range, but at length scales of the order of 500 nm, limited by the wavelength of the light.

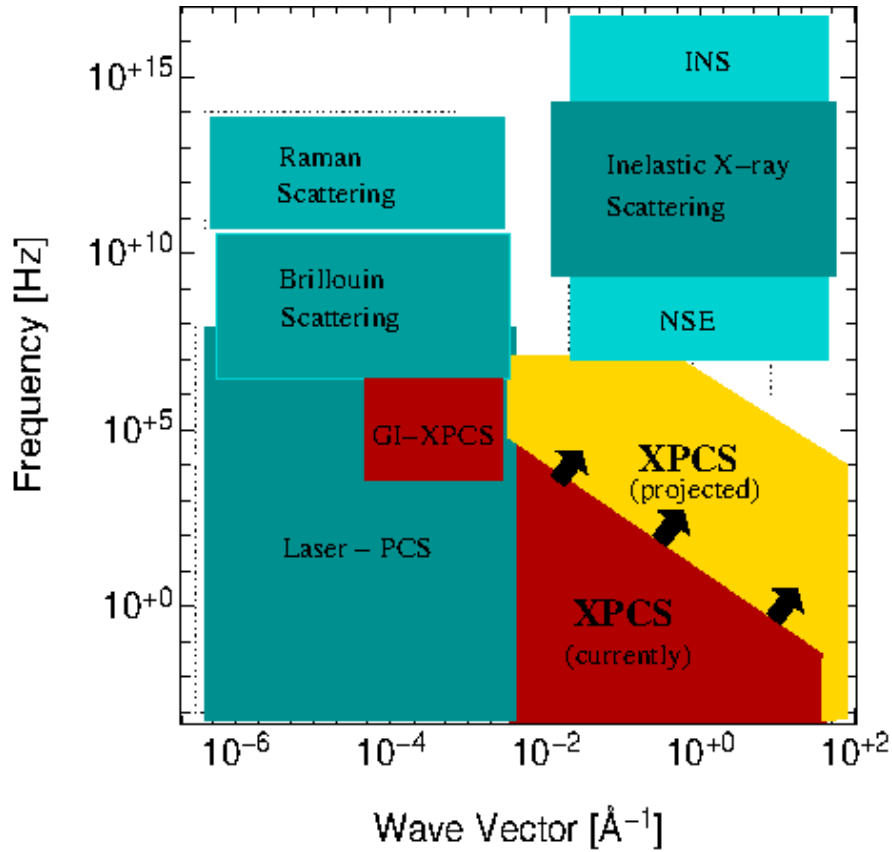


**Figure 1:** Scheme of the space/time regime covered by different techniques: X-ray photon correlation spectroscopy (XPCS) photon correlation spectroscopy with visible coherent light (LPCS), Raman and Brillouin scattering, inelastic neutron (INS) and inelastic X-ray scattering (IXS), neutron spin-echo and nuclear forward scattering (NFS)

For polymer materials this spatial scale is extremely large, and the technique is only useful to study polymer dynamics in few limited systems such as polymer solutions [6, 7] or extremely long molecular weight block copolymers.[8-10] Also, the technique is limited to transparent samples. The possibility of performing similar experiments with X rays has been hindered in the past by the lack of coherence of X ray beams. Synchrotrons are chaotic light sources and do not generate coherent (in space or time) wavefronts. However, with third generation high brightness (photon density in the phase space) synchrotron sources, it has been found that by spatial filtering through appropriate slits and pinholes in the beam path, and temporal filtering by using a monochromator,

coherent X rays can be obtained. Unfortunately, this spatial and temporal filtering comes at a price and leads to important losses of intensity [11], but the high brightness synchrotron radiation (SR) sources can nevertheless be used for X-ray Photon Correlation Spectroscopy (XPCS), the analogue of LPCS with important applications in the study of the nanoscale dynamics of materials and in particular, in the study of polymer and other soft materials, as discussed below.

Figure 1 shows a map of techniques with emphasis on the temporal and spatial scale that LPCS, XPCS and other scattering techniques can resolve.

The spatial coherence of a photon beam is determined by the number of Gaussian “coherent modes” it contains. This is most conveniently quantified using a “phase-space” description of the source properties. For a monochromatic Gaussian source with wavelength  $\lambda$ , “one-sigma” source size  $\sigma$  and angular size  $\sigma'$ , which contains by definition one coherent mode, the phase-space volume is given by [12]:

$$\sigma\sigma' = \frac{\lambda}{4\pi}. \quad (1)$$

This is essentially a diffraction limited coherent source. It thus follows that for a partially coherent source (such a SR source) with one-sigma size and angular size  $\sigma, \sigma'$  the phase-space volume is larger (i.e. the beam contains more coherent modes or, equivalently, is less coherent) and we have a “Heisenberg-like” inequality [12]

$$\sigma\sigma' \geq \frac{\lambda}{4\pi}. \quad (2)$$

It turns out that an equivalent of Liouville’s theorem holds and the phase-space volume of a beam is conserved by propagation, refraction, reflection, etc. which essentially means that the coherence of e.g. a SR beam is essentially a property of the source. The spatial filtering mentioned above consists in using only a part of the phase space volume and hence “throwing away” the remaining flux. One common scheme achieving that is through e.g. a set of slits limiting the angular size of the source. The size that such slits should have in order to provide a (often partially) coherent beam can define a coherence length in the horizontal and vertical direction,  $\xi_h$  and  $\xi_v$ . Simple geometrical arguments lead to [11]:

$$\xi_h = \frac{\lambda R}{4\pi\sigma_h}; \quad \xi_v = \frac{\lambda R}{4\pi\sigma_v} \quad (3)$$

where  $\lambda$  the light wavelength,  $\sigma_h$  and  $\sigma_v$  the (one-sigma) size of the source in the vertical and horizontal direction respectively, assuming a rectangular source, and  $R$  the distance from the source to the sample. Therefore, the further away from the source, the larger the transverse coherence length will be.

Regarding the temporal coherence  $\xi_l$ , often called longitudinal coherence, this magnitude is inversely proportional to the bandwidth. Assuming a Lorentzian temporal spectrum, the expression for  $\xi_l$  is given by [11]:

$$\xi_l \approx (2/\pi) \lambda^2 / \Delta \lambda \quad (4)$$

Because of expression (4), an extremely well monochromatized beam should be obtained in order to maximize  $\xi_l$ .

With the transverse and longitudinal coherence lengths defined above, the coherent flux will be measured by the number of photons/s in a coherence volume  $V = \xi_h \xi_v \xi_l$ . Again, simple geometrical arguments lead to

$$F = B \lambda^2 \frac{\Delta \lambda}{\lambda} \quad (5)$$

where the important quantity that was introduced is B, the source brilliance which measures the number of photons per unit of time generated from the source per unit of source area per unit solid angle and per 0.1% fractional band width.[11]. In third generation synchrotrons, B is higher than  $10^{20}$  photons  $s^{-1}$   $mm^{-2}$   $mrad^{-2}$   $(0.1\% \text{ BW})^{-1}$  for photon energies around 8 keV allowing coherent scattering experiments to be performed. It should also be mentioned that at the most recent SR sources the brightness will be higher by more than one order of magnitude (or even several orders of magnitude, at lower energies) and this will lead to a tremendous expansion of the time scales accessible to XPCS. Indeed, the signal-to-noise ratio of the correlation functions measured by XPCS scales linearly with the source brightness but only with the power  $1/2$  of the shortest measured correlation time. As a consequence, an increase in the source brightness by one order of magnitude enables measurements with the same signal-to-noise ratio of dynamics 100 times faster. This fact is highlighted by the “projected” XPCS area in the phase space shown in Figure 1.

Nowadays, the number of beamlines offering coherent light in synchrotrons is growing, not only for XPCS experiments but also other techniques are emerging that take profit of the possibility of selecting a part of the beam with the appropriate coherence characteristics. Table 1 shows a review of the operative coherent X ray beamlines that offer XPCS and the techniques available in them.

Beamline	Synchrotron Source	Country	Status	Technique
ID10CS	ESRF	France	Operative	XPCS/CXD
8-ID	APS Argonne	USA	Operative	XPCS
BL40_XU	SPring-8	Japan	In operation	XPCS/CXD
P10	Petra-III	Germany	In operation	XPCS/CXD

CHX (11-ID)	NSLS-II	USA	Comissioning	XPCS/CXD
-------------	---------	-----	--------------	----------

Table 1: List of some of the operative X-Ray beamlines that offer XPCS techniques. Some of them offer also Coherent X-ray Diffraction Imaging (CXD)

### A typical XPCS experiment. How does it work?

When a coherent light beam interacts with a disordered system, the beam is scattering giving rise to a random diffraction or “speckle” pattern. The speckle pattern is related to the precise spatial arrangement of the disordered scatterers. The pattern can be then interpreted as the instantaneous diffraction pattern of the disordered system. If the same experiment is performed with a non-coherent light beam, instead of the speckle pattern, an average over ‘many’ speckle patterns is observed. In an XPCS experiment a ‘movie’ is built by consecutive collection of an enough quantity of those instantaneous images. By analyzing how the intensity at a given position on the detector, i.e, at a given value of the  $q$  vector, varies from frame to frame, a intensity time-correlation curve can be obtained. Mathematically,

$$g_2(q, t) = \frac{\langle I(q, 0)I(q, t) \rangle}{\langle I(q, t) \rangle^2} \quad (6)$$

Where  $q = (4\pi/\lambda)\sin(\theta)$  with  $2\theta$  the scattering angle and  $\langle \rangle$  denotes an ensemble averaged performed in this case of all equivalent times and possibly all equivalent pixels of an area detector.

A schematic view of such an experiment is presented in figure 2.

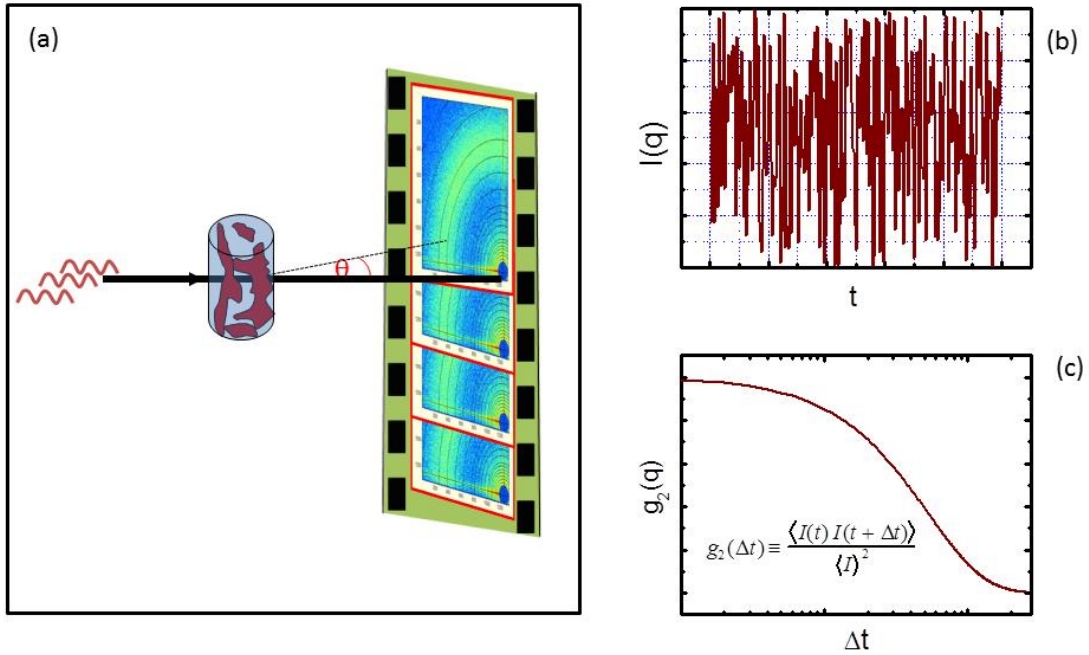


**Figure 2:** Scheme of an XPCS experiment. A partly coherent X ray beam interacts with a disordered sample, giving rise to an scattering speckle patterns. The distribution of speckles will depend on the exact position of the scatterers in the sample at a given time. In (a) the consecutive collection of such patterns provides information on the dynamical variation

of the position of those scatterers. (b) represents the temporal intensity variations at a particular  $q$  vector. In (c), the autocorrelation function of the intensity shown in (b) is presented.

The characteristics decay times of  $g_2(q,t)$  will correspond to characteristics relaxation times of the relevant dynamics (density fluctuations) of the system over the studied  $q$ -range. In other words, XPCS reveals the stochastic evolution of the disorder in a sample at the length scale related to the observed scattering vector.

## **History of XPCS experiments and variety of investigated systems.**

In 1991, Sutton et al observed a speckle pattern from randomly arranged antiphase domains in a single crystal of the binary alloy  $\text{Cu}_3\text{Au}$  using coherent X rays. [13] These experiments were performed at the beamline X25 at NSLS in Brookhaven National Laboratory. The first XPCS experiments demonstrating the feasibility of observing the motions of microstructures in polymer blends or colloidal systems were performed in 1995 by B. Chu et al. [14] at the X3 beamline and by Dierker et al. [15] at the same X25 beamline, both at NSLS. From that moment, XPCS experiments started to be reported mainly in the field of colloidal motions in concentrated samples [16-19], experiments unfeasible by PCS until that date due to high absorption and/or multiple scattering. Light scattering experiments were developed in parallel, to circumvent the problem of multiple scattering via cross correlations techniques using two colors and two (scattering) angles. [20, 21] While in the low volume fraction limit, the motion of colloids in a solvent is well described by a single particle Brownian model, at high concentration complex many-body effects emerge as a result of direct interparticle interactions as well as indirect hydrodynamic interactions mediated by the solvent. The advances in LPCS and XPCS allowed the study of such systems and in several cases, a direct comparison between the two techniques. For instance, from a two-color LPCS experiment performed on sterically-stabilized hard-sphere colloids, Segre and Pusey found that the short and long time diffusion coefficients scale with the structure factor [22]. However, Lurio et al. [19] questioned these results after performing XPCS experiments on charge-stabilized polystyrene latex spheres in glycerol and concluding that the long time scaling was different from that observed at short times. More recently, in a work which combined both LPCS and XPCS, Martinez et al. [23] demonstrated that both techniques deliver the same results, as shown in Figure 3, where the intermediate scattering function, that is, the Fourier transform of the time and space dependent pair distribution function, [24] obtained from the autocorrelation of the intensity is presented. Surprisingly, while confirming the scaling of the short-time diffusion coefficient with the static structure factor, the study of Martinez et al. [23] found no evidence of a collective long time diffusive regime.

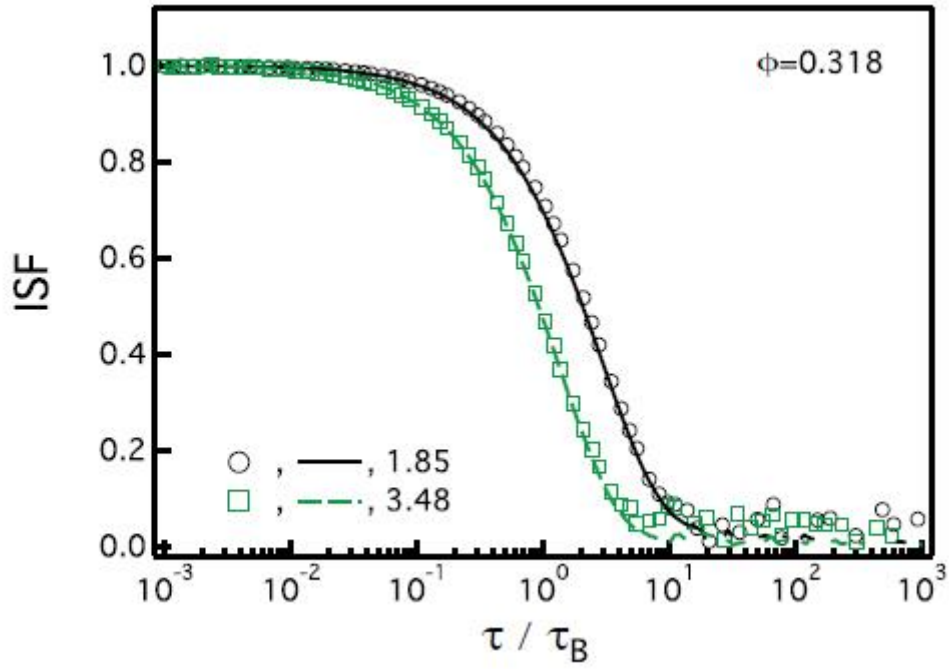


**Figure 3.** Intermediate Scattering Function of a colloidal hard sphere system of radius  $R=185\text{nm}$ , obtained from XPCS (open symbols) and light photon correlation spectroscopy LPCS (lines) at a given volume fraction and  $qR$  values indicated. Adapted from [23] with permission.

The dynamics of concentrated hard-sphere suspensions was further studied using XPCS by Orsi et al. [25] where the authors established the limits of validity of the “Segre-Pusey scaling” [22] between the short-time and long-time diffusion coefficients mentioned above and compared their results both with theoretical predictions by the Mode Coupling Theory or numerical simulations as well as with the experimental results of Martinez et al. [23].

In a subsequent investigation by Kwasniewski et al. [26], the concentration of the hard-sphere suspensions were further increased towards the putative “colloidal glass transition” where the long-time diffusion becomes infinite and the suspension is expected to arrest in a non-ergodic glass phase. However, the authors did not observe such a transition as the samples remained ergodic even above the glass transition concentration. At the same time, they observed the onset of anomalous hyperdiffusive relaxation modes and deviations from theoretical predictions leading them to propose that at those concentrations, a new, non-thermal and most-likely stress-induced, relaxation mechanism appears and restores ergodicity.

With the aim of investigating fluctuations arising from the glass transition in undercooled liquids, and with the idea of increasing the X ray contrast, the dynamics of nanoparticles in an undercooled liquid was also studied by XPCS. [27, 28] In these studies it was observed that while at temperatures well above the glass transition the particles undergo Brownian motion, at temperatures close to the glass transition the dynamics of the particles became hyperdiffusive. XPCS has been extended to study bulk dynamics in more complex systems like lamellar phases in lyotropic systems [29],

magnetic colloids [30-32] suspensions of nanometer-sized clay disks [33-35] depletion gels [36] and polymer systems, as will be described below.

The development of XPCS opened the possibility of performing experiments in grazing incidence geometry, and therefore by choosing the incident angle, being selective on the depth of the sample to be explored. By selecting angles below the critical angle for total external reflection, the region studied corresponds just to a few nanometers into the surface. In such condition, the fluctuations on the surface are probed. On the other hand, by increasing the incidence angle, the X Ray beam penetrates into a larger portion of the sample and the inner dynamics is probed. In this way, overdamped capillary waves in undercooled glycerol surfaces [37] were detected and the behavior of them was described by using the bulk viscosity value, indicating that viscosity at the surface is not that different from that of the bulk material. Other studies on capillary waves in different liquids and liquid mixtures [38, 39] followed, showing the versatility of the XPCS in this field and the experiments were extended to complex systems like membranes [40] and polymers, as will also be described below.

## **XPCS experiments on polymers**

### **Dynamics of polymers by XPCS using tracers.**

The glass transition phenomena is one of the most studied problems in polymer dynamics. XPCS in principle matches the time scale for the relevant modes that appears at temperatures above the glass transition. However, due to the weakness of the scattering signal at the position of the structure factor peak, it is not possible to study the dynamics in neat polymers, in the same way as it is not possible to do it in neat liquids. Therefore, the use of particles as tracers for the matrix dynamics, in low enough concentration to avoid particle particle interactions, is the approach of choice for these experiments. In this way, similarly to the approach mentioned above by Caronna et al. [27] for the dynamics of propanediol, gold nanoparticles were used as tracers in low molecular weight polystyrene to study the polymer dynamics above its glass transition temperature ( $T_g$ ) [41], where a transition from a diffusive motion of the nanoparticles at high temperatures to a hyperdiffusive behavior closer to  $T_g$  has been observed as well. The crossover between one and the other behavior is found to be around  $1.1T_g$ . Similarly, Hoshino et al. [42] performed XPCS experiments on atactic polystyrene melts using polystyrene grafted silica particles as tracers. The idea behind using these peculiar tracers is to increase the interaction between the tracer and the polymer matrix. They obtain a crossover temperature of about  $1.25T_g$ . The intensity-intensity autocorrelation function  $g_2$  expressed in equation (5) can be described by an exponential like function in the form:

$$g_2(q, t) = \beta \exp[-2(\Gamma t)^\nu] + 1 \quad (7)$$



At high temperatures,  $g_2$  can be described by a stretched exponential ( $\gamma < 1$ ), whereas below the crossover,  $g_2$  is described by a compressed exponential ( $\gamma > 1$ ) (see figure 4). The authors attribute the sub-diffusive behavior observed at high temperatures to the nanoparticles moving in a more constrained way than simple Brownian diffusion due to the entanglement effect of the polymer matrix and the chains attached to the nanoparticles.

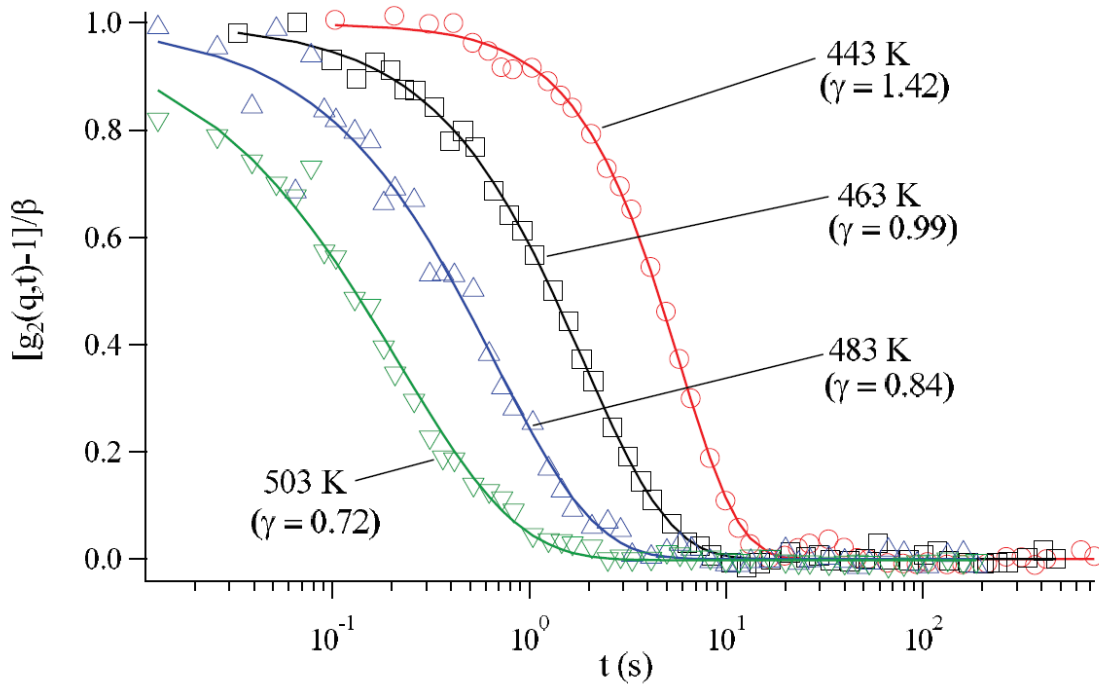


Figure 4. Normalized autocorrelation functions (symbols) measured at  $q = 2.15 \times 10^{-2} \text{ nm}^{-1}$  for the PS-grafted nanoparticles dispersed in a PS matrix at different temperatures. Solid lines are fitting curves for Eq. 5. Reprinted from [42] with permission of the American Physical Society

The idea of the tracers was applied to investigate the role of filler–filler and the filler–matrix interactions in a cross-linked elastomer on the aging mechanisms under strain. [43] They used carbon black as filler, which presents a strong matrix-filler interactions, or hydroxylated silica that interact with each other via H-bonding. In both cases the results revealed signatures of a jammed dynamics with compressed exponential and ballistic motion, although the exponents characterizing the aging were different in one and the other cases. Shinohara et al. [44] investigated the dynamics of silica particles in unvulcanized rubber and studied the aging behavior of the dynamics. They show that particles dynamics was slowing down with increasing aging time. This slowing down was not due to aggregation of the filler, and it did depend on the volume fraction of silica particles.

Also, the gelation dynamics of a biopolymer has been studied by XPCS using silica nanoparticles as tracers.[45] In that work the authors found a stress-dominated dynamics as the system approached the gel state, characterized by a hyper-diffusive motion of the silica particles.

More recently, the question on whether the filler or nanoparticles, more generally, the tracers, shows the same dynamics as the matrix has been tackled by studying by XPCS the slow dynamics of aerogels and nanocomposite aerogels.[46] In that work both aerogels formed through freezing-drying of semi-interpenetrating polymer networks of alginate and poly(N-isopropylacrylamide) and nanocomposite of the same aerogels with iron oxide NPs present hyperdiffusive dynamics. The observed dynamics arises from the porous structure and not from the presence of the nanoparticles. However, polymer aerogel nanocomposites exhibited longer relaxation times due to the interactions of the polymer chains with the nanoparticles.

The same aerogels can be hydrated and form thermosensitive hydrogels that show a reversible hydration–dehydration change in response to small temperature changes around its lower critical solution temperature (LCST). Above LCST, the polymer gel collapses.[47] Because of the release of hydrophobic hydration, the LCST transition leads to dramatic changes in physical properties, such as mechanical, optical, and thermal properties. The hydrogels [48] exhibited a hyper-diffusive dynamics of similar nature as that found for the freeze-dried aerogels which had been attributed to their characteristic porous structure. The dynamics of the swollen samples was found to be faster than that of the freeze-dried ones suggesting that water has an effect in accelerating the dynamics of the hydrogels. Again in this case the presence of the iron nanoparticle is to slow down the observed relaxation. Regardless of the presence of the nanoparticles, the relaxation becomes slower as the gel deswelled. This fact can be inferred by observing the two-time correlation function  $G(q, t_1, t_2)$  (see figure 5).

$$G(q, t_1, t_2) = \frac{\langle I(q, t_1)I(q, t_2) \rangle}{\langle I(q, t_1) \rangle \langle I(q, t_2) \rangle} = \beta \exp[-2(\Gamma t)^\nu] + 1 \quad (8)$$

The variables describing the two-time correlation function are the average time or age,  $t_a = (t_1 + t_2)/2$ , measured by the distance along the  $t_1 = t_2$  diagonal and the time difference  $t = t_1 - t_2$ , which is the distance from the  $t_1 = t_2$  diagonal in the perpendicular direction.

At temperatures below LCST, the iso-intensity lines in plots  $G(q, t_1, t_2)$  show a decrease in the width perpendicular to the diagonal which indicates shorter characteristic times of the dynamics of the samples at these temperatures. Above LCST, the width perpendicular to the diagonal is larger indicating a slowing-down of dynamics with aging time. At the LCST ( $T = 32^\circ\text{C}$  for this system) the two time correlation function depend only on the time difference  $t$ , and hence the two time correlation contour lines are parallel which is indicative of stationary dynamics.

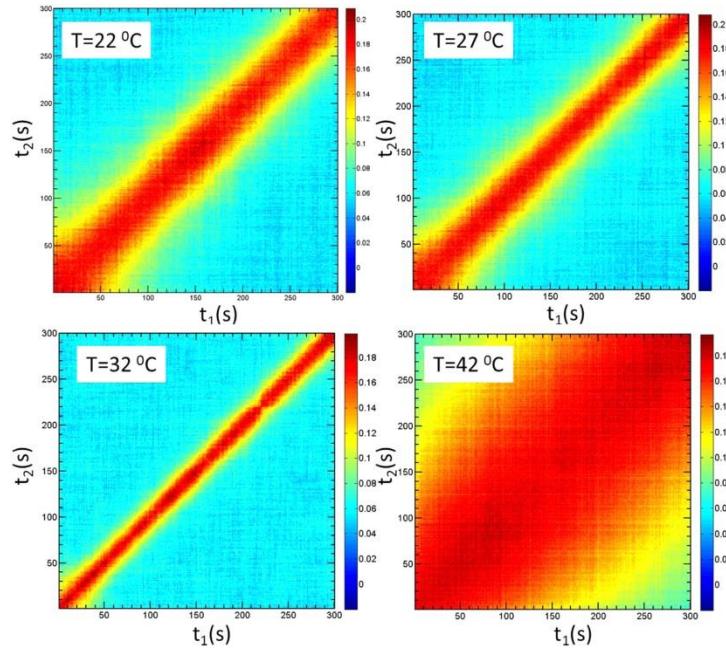


Figure 5: Two-time correlation function  $G$  ( $q = 0.0439 \text{ nm}^{-1}$ ,  $t_1, t_2$ ) obtained for a nanocomposite hydrogel at different temperature, below, at and above the LCST. Reprinted from [48] with permission from the American Chemical Society.

The deswelling dynamics was also studied by XPCS in the case of hydrogels of poly(N-isopropyl acrylamide) [49, 50], where a compressed exponential decay and hyper-diffusive dispersion relationships were observed. The results show that the relaxation time below and above the LCST follows a  $q^{-1}$  dependence, characteristic of jammed systems.

Very recently also the dynamics of polymeric nanocolloids moving through a highly viscous polymer matrix have been studied by XPCS. [51] The authors have observed an unusually large reduction of effective viscosity experienced by polymeric nanocolloids at temperatures well above the  $T_g$  of the matrix. The extent of reduction in effective interface viscosity increases with decreasing temperature and polymer film thickness.

### **XPCS experiments in block copolymers and blends.**

Inspired by the studies of diffusion of nanoparticles in liquids by XPCS, in the late nineties, Mochrie and coworkers published a work on the dynamics of block copolymer micelles in a homopolymer matrix [52] where they found a wave-vector dependent inverse diffusion coefficient, in the case of both, spherical and worm like micelles. Yet, experiments on the dynamics of entangled polymer melts were reported [53], where, by XPCS, the authors studied the dynamics of compositional fluctuations and obtained that the measured relaxation times were consistent with predictions of the reptation model. Those works opened the road for investigating the dynamics on polymer self-assembled systems [54-56], from which, block copolymers are the more suitable since their structure had been intensively studied by Small Angle X Ray Scattering (SAXS)[57].

In any two polymer mixtures A and B, either blends A/B or A-B block copolymers, composition fluctuations are behind the transition from the homogeneous-mixed state to the phase separated

one, and this is evidenced by a maximum in the static structure factor  $S(q)$  at a finite value of the wave vector modulus  $q^*$ . The dynamics of such a transition from mixed to phase separated state in block copolymer have been described by the mean field theory for incompressible systems. The theory initially predicts that composition fluctuations relax via an internal chain mode, often called breathing mode with a relaxation rate that is independent of  $q$ . This mode arises from the relative translational motion of the center of mass of the blocks. Arising from the heterogeneity of composition along the chain another mode of diffusive character, and therefore showing a  $q^2$  dependence is predicted.[7] These mode were extensively studied by LPCS in the nineties [7, 58-62], in block copolymer solution and in very large molecular weight block copolymer melts. Patel et al. [63] observed by XPCS a structural relaxation in disordered block copolymer melts that slowed down as the system is cooled down and it approaches the temperature of transition from disorder to order ( $T_{DOT}$ ). They consider that this observed relaxation arises from the diffusion of micelles in the block copolymer melt. Later, the same group investigated the dynamics by XPCS on samples quenched from disorder-to-order [64] and observed that the microscopic relaxation time, measured by XPCS, increases after all quenches, whereas only deep quenching into the order region produced evidences of ordering by other techniques like SAXS and rheology. They explained these observations by postulating the presence of nucleation barriers for the ordered phase. Recently, the slowing down of the breathing mode as the transition from disorder to order is approached has been also demonstrated by XPCS in diblock copolymers that exhibit a lower disorder-order temperature, i. e. systems that exhibits phase separation upon heating [65]. In that case, two different modes have been observed. At temperatures below the disorder to order transition, a non-diffusive mode appears, associated with compositional fluctuations. This mode that becomes slower as the interaction parameter increases, in a similar way to the one observed for diblock copolymers exhibiting phase separation upon cooling. Above  $T_{DOT}$ , the dynamics becomes diffusive; indicating that after phase separation the diffusion of chain segments across the interface is the governing dynamics. As the segregation is stronger (higher temperatures), the diffusive process becomes slower (Figure 6).

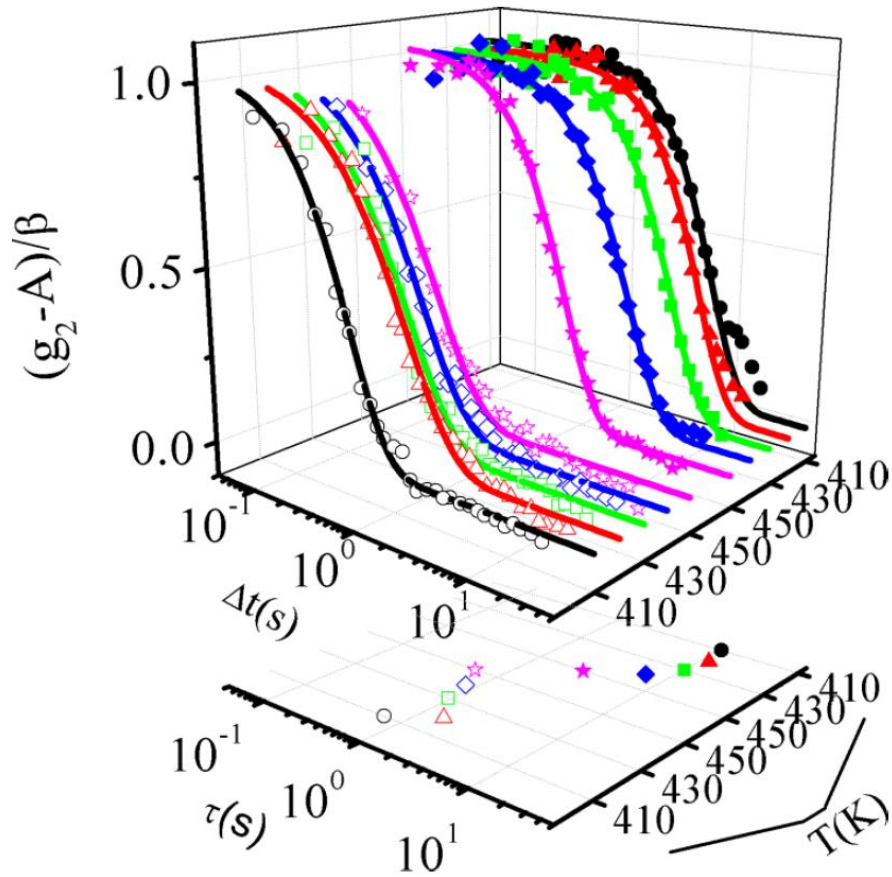


Figure 6: Intensity-intensity autocorrelation function as a function of the elapsed time, obtained at the value  $q^*$  of the structure factor maximum at different temperatures, upon heating from the homogeneous state (open symbols), and during subsequent cooling (filled symbols) at different temperatures. In the bottom panel, the characteristic relaxation time is presented as a function of temperature. Reprinted with permission from [65].

It is worth pointing out that at the ordered or phase separated state, the autocorrelation function has a compressed exponential shape. This sort of exponential, that was also observed in polymer hydrogels and polymer aerogels[46, 48-50] appeared in multicomponent polymer blends [66] at low temperatures. In both cases, this is an indication of jammed dynamics, since always appears in the situation where the dynamics is more crowded, i. e. lower temperatures in glassy systems and in the phase separated state in block copolymers and blends.

### Experiments on polymers in grazing incidence geometry.

The study of capillary waves in thin polymer films by XPCS is relatively easy to tackle by using grazing incidence geometry since capillary waves in polymers, due to their high viscosity, present a slow motion that can be followed by slow-readout detectors. Kim et al. [67] studied, by XPCS, the surface dynamics on thin polystyrene films above the glass transition temperature. They described the measured surface dynamics by the theory of overdamped thermal capillary waves on thin viscoelastic films. Also, the data allowed them to obtain viscosity data that agreed with those of bulk PS. However, as the thickness of the film is decreased to dimensions comparable to the radius of gyration of the polymer, the conventional model of capillary waves on viscous liquids cannot

explain properly the results observed by XPCS [68] and the effects of pinning of the polymer to the surface should be included. Following this idea, XPCS in Grazing Incidence Geometry has been used to elucidate the role of substrates on the surface wave relaxation times [69]. That work revealed that the dynamics of a polymer can be greatly affected by a neighboring immiscible system, especially close to the  $T_g$  of the polymer and that this effect can extend over large length scales, larger than those characteristic of the segmental dynamics, or even more, the polymer radius of gyration. In systems with molecular weight large enough to present entanglements, Jiang et al. studied by XPCS capillary waves dynamics at temperatures well above  $T_g$ , where they observe a single exponential decay that attribute to chain reptation, whereas at temperatures close to  $T_g$  they found a more local motion, that they identifies as Rouse dynamics.[70] These studies have been recently extended to polymers with different molecular architectures[71].

Recently studies of XPCS in grazing incidence geometry on nanoparticles-phospholipid layers have been published. [72] This study has biological relevance since the studied systems can be considered as model for nanoparticle diffusion through membranes

The motion of tracers in buried systems have been recently followed by XPCS by Koga et al.[73] Through this method they obtained the viscosity of the free surface and found it to be about 30% lower than the bulk viscosity, attributing this decrease to the reduced number of entanglements in the surface. Grazing incidence geometry opens the door to the study of buried surfaces in multilayers systems.

Yet XPCS has been employed to explore the in-plane dynamics of a buried interface in a polymeric bilayer [74], showing that its dynamics is similar to the slower mode dynamics observed at the top surface (i.e. at the polymer/vacuum interface).

Another physical aspect of thin liquids layers in general and polymers in particular is wetting. It is known that wetting depends on the substrate topography. Recently, XPCS have been used to assess the surface dynamics of thin molten polystyrene films supported by periodically nanostructured silicon surfaces.[75] The authors probed that the surface dynamics on these nanostructures was highly anisotropy at certain length scales due to the substrate nanostructuration. Their results also probe the effect of topologic confinement on capillary waves and this technique can be used to investigate the effect of it on polymer-surface interactions.

XPCS experiments performed under this geometry have been recently reviewed by Sinha et al. [76]

## **Perspectives of XPCS in polymers science**

The examples depicted above show that XPCS technique applied to polymer science is at the beginning of its way, and that offers a wide variety of possibilities to study dynamic in polymers under different situations. The fact that new lines are being commissioned at the moment will

provide future opportunities to performing experiments with complex sample environment, some of them are already being tested [77]. One of the limiting issues in XPCS is related to the radiation damage. The development of new sources that provides higher coherent fluxes, however, would also enhance this limiting aspect. However, there is hope, since in the last decade it was proved that it is possible to perform XPCS experiments using higher energy X-rays [78], that exhibit lower absorption and therefore radiation damage is reduced. However, this benefit is obtained as expenses of the decrease in the coherent flux, since it scales with the square of the wavelength (see equation 5), and therefore, high energy experiment shows a decrease in the signal to noise ratio that impedes its use in most of the cases. With the advent of new low emittance storage, where the brightness and coherent fraction of the beam are expected to increase by orders of magnitude [79], the targets of XPCS experiments will immediately boost. The increase of the coherent fraction will allow XPCS measurements at much higher energies than possible today. In parallel to the reduced radiation damage, the lower absorption permits the use of thicker samples, increasing the signal-to-noise ratio. All these aspects represent new opportunities for studying polymer systems where low contrast is observed, like dynamics of homopolymer melts and polymers in solution, dynamics during polymerization processes etc.

Yet, the development of X Ray Free Electron Lasers (XFEL) will enhance the possibility of measuring dynamics at very short times down to the femtoseconds scale. This is possible because the coherent intensity of XFEL sources within a single lasing pulse of time length of the order of tenths of picoseconds is comparable to the average figures obtained at third generation synchrotrons. However, although XFELs are opening completely new and unexplored scientific areas thanks to their unprecedented flux, coherence, and time structures, the problem of radiation damage, which it is also present in third generation synchrotron sources, [80] is a major concern. Recent experiments on the dynamics of gold nanoparticles on a polymer melts suggest that the X ray induced damage and heating are less harmful than initially expected. [81] Still, several experimental strategies have been proposed for minimizing the effect of radiation at XFELs. One of them is based on single shots with an extremely high photon flux in a small beam size, what it is known as “diffract before destroy” regime, where the sample is irreversibly damaged but the experiment information is obtained before destruction.[82] Another approach, consists of—using medium photon fluxes and beam sizes, assuring that the sample can survive for at least a few pulses, and damage is occurring only on a (small) spatial extent still compatible with the experiment. Such approach will require the ability to change the illuminated volume, e.g. by using a flow device. All these methodologies are currently under development and their success will widen the possibility of measuring dynamics in polymer systems on (shorter) time and (smaller) length scales that are inaccessible today.

## Acknowledgements

The authors gratefully acknowledge financial support from the MINECO (MAT2014-59187-R) and from NSLS-II under contract No. DE-SC0012704 with the US Department of Energy.

## REFERENCES

1. Koenig, J.L., *Chapter 4 - Applications of IR spectroscopy to polymers*, in *Spectroscopy of Polymers (Second Edition)*, J.L. Koenig, Editor. 1999, Elsevier Science: New York. p. 147-206.
2. Koenig, J.L., *Chapter 5 - Raman spectroscopy of polymers*, in *Spectroscopy of Polymers (Second Edition)*, J.L. Koenig, Editor. 1999, Elsevier Science: New York. p. 207-254.
3. Kremer, F. and A. Schonhals, eds. *Broadband Dielectric Spectroscopy*. 2002, Springer Verlag: Heidelberg.
4. Colmenero, J. and A. Arbe, *Recent progress on polymer dynamics by neutron scattering: From simple polymers to complex materials*. Journal of Polymer Science Part B: Polymer Physics, 2013. **51**(2): p. 87-113.
5. Berne, B.J. and R. Pecora, *Dynamic Light Scattering*. 2000, New York: Dover Publications Inc.
6. Chu, B. and D.C. Lee, *Characterization of poly(methyl methacrylate) during the thermal polymerization of methyl methacrylate*. Macromolecules, 1984. **17**(4): p. 926-937.
7. Semenov, A.N., et al., *Dynamic Structure Factor of Diblock Copolymers in the Ordering Regime*. Macromolecules, 1997. **30**(20): p. 6280-6294.
8. Fytas, G., et al., *Local and global chain dynamics in diblock copolymer melts*. Physica Scripta, 1993. **1993**(T49A): p. 237.
9. Anastasiadis, S.H., et al., *Breathing and composition pattern relaxation in "homogeneous" diblock copolymers*. Physical Review Letters, 1993. **70**(16): p. 2415-2418.
10. Anastasiadis, S.H., et al., *Diffusive Composition Pattern Relaxation in Disordered Diblock Copolymer Melts*. EPL (Europhysics Letters), 1993. **22**(8): p. 619.
11. Friso van der, V. and P. Franz, *Coherent x-ray scattering*. Journal of Physics: Condensed Matter, 2004. **16**(28): p. 5003.
12. Wiedemann, H., *Synchrotron Radiation*. Advanced Texts in Physics. 2003: Springer-Verlag Berlin Heidelberg.
13. Sutton, M., et al., *Observation of speckle by diffraction with coherent X-rays*. Nature, 1991. **352**(6336): p. 608-610.
14. Chu, B., et al., *AN X-RAY PHOTON-CORRELATION EXPERIMENT*. Langmuir, 1995. **11**(5): p. 1419-1421.
15. Dierker, S.B., et al., *X-RAY PHOTON-CORRELATION SPECTROSCOPY STUDY OF BROWNIAN-MOTION OF GOLD COLLOIDS IN GLYCEROL*. Physical Review Letters, 1995. **75**(3): p. 449-452.
16. Thurn-Albrecht, T., et al., *Photon Correlation Spectroscopy of Colloidal Palladium Using a Coherent X-Ray Beam*. Physical Review Letters, 1996. **77**(27): p. 5437-5440.
17. Tsui, O.K.C. and S.G.J. Mochrie, *Dynamics of concentrated colloidal suspensions probed by x-ray correlation spectroscopy*. Physical Review E, 1998. **57**(2): p. 2030-2034.
18. Thurn-Albrecht, T., et al., *Structure and dynamics of surfactant-stabilized aggregates of palladium nanoparticles under dilute and semidilute conditions: Static and dynamic x-ray scattering*. Physical Review E, 1999. **59**(1): p. 642-649.
19. Lurio, L.B., et al., *Absence of Scaling for the Intermediate Scattering Function of a Hard-Sphere Suspension: Static and Dynamic X-Ray Scattering from Concentrated Polystyrene Latex Spheres*. Physical Review Letters, 2000. **84**(4): p. 785-788.
20. Pusey, P.N., *Suppression of multiple scattering by photon cross-correlation techniques*. Current Opinion in Colloid & Interface Science, 1999. **4**(3): p. 177-185.
21. Scheffold, F. and R. Cerbino, *New trends in light scattering*. Current Opinion in Colloid & Interface Science, 2007. **12**(1): p. 50-57.



22. Segrè, P.N. and P.N. Pusey, *Scaling of the Dynamic Scattering Function of Concentrated Colloidal Suspensions*. Physical Review Letters, 1996. **77**(4): p. 771-774.
23. Martinez, V.A., et al., *Dynamics of hard sphere suspensions using dynamic light scattering and X-ray photon correlation spectroscopy: Dynamics and scaling of the intermediate scattering function*. The Journal of Chemical Physics, 2011. **134**(5): p. 054505.
24. Van Hove, L., *Correlations in Space and Time and Born Approximation Scattering in Systems of Interacting Particles*. Physical Review, 1954. **95**(1): p. 249-262.
25. Orsi, D., et al., *Dynamics in dense hard-sphere colloidal suspensions*. Physical Review E, 2012. **85**(1): p. 011402.
26. Kwasniewski, P., A. Fluerasu, and A. Madsen, *Anomalous dynamics at the hard-sphere glass transition*. Soft Matter, 2014. **10**(43): p. 8698-8704.
27. Caronna, C., et al., *Dynamics of Nanoparticles in a Supercooled Liquid*. Physical Review Letters, 2008. **100**(5): p. 055702.
28. Conrad, H., et al., *Correlated heterogeneous dynamics in glass-forming polymers*. Physical Review E, 2015. **91**(4): p. 042309.
29. Constantin, D., et al., *Dynamics of bulk fluctuations in a lamellar phase studied by coherent x-ray scattering*. Physical Review E, 2006. **74**(3): p. 031706.
30. Lal, J., et al., *Dynamics and correlations in magnetic colloidal systems studied by X-ray photon correlation spectroscopy*. The European Physical Journal E, 2001. **4**(3): p. 263-271.
31. Robert, A., et al., *Structure and dynamics of electrostatically interacting magnetic nanoparticles in suspension*. The Journal of Chemical Physics, 2005. **122**(8): p. 084701.
32. Wandersman, E., et al., *Field induced anisotropic cooperativity in a magnetic colloidal glass*. Soft Matter, 2015. **11**(36): p. 7165-7170.
33. Bandyopadhyay, R., et al., *Evolution of Particle-Scale Dynamics in an Aging Clay Suspension*. Physical Review Letters, 2004. **93**(22): p. 228302.
34. Angelini, R., et al., *Glass-glass transition during aging of a colloidal clay*. Nat Commun, 2014. **5**.
35. Augusto de Melo Marques, F., et al., *Structural and microscopic relaxations in a colloidal glass*. Soft Matter, 2015. **11**(3): p. 466-471.
36. Fluerasu, A., et al., *Slow dynamics and aging in colloidal gels studied by x-ray photon correlation spectroscopy*. Physical Review E, 2007. **76**(1): p. 010401.
37. Seydel, T., et al., *Capillary waves in slow motion*. Physical Review B, 2001. **63**(7): p. 073409.
38. Madsen, A., et al., *Capillary Waves at the Transition from Propagating to Overdamped Behavior*. Physical Review Letters, 2004. **92**(9): p. 096104.
39. Sloutskin, E., et al., *Dynamics and critical damping of capillary waves in an ionic liquid*. Physical Review E, 2008. **77**(6): p. 060601.
40. Sikharulidze, I., et al., *Surface and Bulk Elasticity Determined Fluctuation Regimes in Smectic Membranes*. Physical Review Letters, 2003. **91**(16): p. 165504.
41. Guo, H., et al., *Nanoparticle Motion within Glassy Polymer Melts*. Physical Review Letters, 2009. **102**(7): p. 075702.
42. Hoshino, T., et al., *Dynamical crossover between hyperdiffusion and subdiffusion of polymer-grafted nanoparticles in a polymer matrix*. Physical Review E, 2013. **88**(3): p. 032602.
43. Ehrburger-Dolle, F., et al., *XPCS Investigation of the Dynamics of Filler Particles in Stretched Filled Elastomers*. Macromolecules, 2012. **45**(21): p. 8691-8701.
44. Shinohara, Y., et al., *Microscopic Observation of Aging of Silica Particles in Unvulcanized Rubber*. Macromolecules, 2010. **43**(22): p. 9480-9487.
45. Ruta, B., et al., *Silica nanoparticles as tracers of the gelation dynamics of a natural biopolymer physical gel*. Soft Matter, 2014. **10**(25): p. 4547-4554.
46. Hernández, R., et al., *Slow dynamics of nanocomposite polymer aerogels as revealed by X-ray photocorrelation spectroscopy (XPCS)*. The Journal of Chemical Physics, 2014. **140**(2): p. 024909.
47. Schild, H.G., *Poly(N-isopropylacrylamide): experiment, theory and application*. Progress in Polymer Science, 1992. **17**(2): p. 163-249.
48. Hernández, R., et al., *Deswelling of Poly(N-isopropylacrylamide) Derived Hydrogels and Their Nanocomposites with Iron Oxide Nanoparticles As Revealed by X-ray Photon Correlation Spectroscopy*. Macromolecules, 2015. **48**(2): p. 393-399.
49. Laszlo, K., et al., *Deswelling kinetics of PNIPAA gels*. Soft Matter, 2010. **6**(18): p. 4335-4338.

50. Geissler, E., et al., *X-ray Photon Correlation Spectroscopy of Dynamics in Thermosensitive Gels*. Macromolecular Symposia, 2007. **256**(1): p. 73-79.
51. Begam, N., et al., *Anomalous Viscosity Reduction and Hydrodynamic Interactions of Polymeric Nanocolloids in Polymers*. Macromolecules, 2015. **48**(18): p. 6646-6651.
52. Mochrie, S.G.J., et al., *Dynamics of Block Copolymer Micelles Revealed by X-Ray Intensity Fluctuation Spectroscopy*. Physical Review Letters, 1997. **78**(7): p. 1275-1278.
53. Lumma, D., et al., *Equilibrium Dynamics in the Nondiffusive Regime of an Entangled Polymer Blend*. Physical Review Letters, 2001. **86**(10): p. 2042-2045.
54. Falus, P., et al., *Symmetric-to-Asymmetric Transition in Triblock Copolymer-Homopolymer Blends*. Physical Review Letters, 2004. **93**(14): p. 145701.
55. Falus, P., M.A. Borthwick, and S.G.J. Mochrie, *Fluctuation Dynamics of Block Copolymer Vesicles*. Physical Review Letters, 2005. **94**(1): p. 016105.
56. Falus, P., et al., *Crossover from Stretched to Compressed Exponential Relaxations in a Polymer-Based Sponge Phase*. Physical Review Letters, 2006. **97**(6): p. 066102.
57. Hamley, I.W. and V. Castelletto, *Small-angle scattering of block copolymers in the melt, solution and crystal states*. Progress in Polymer Science (Oxford), 2004. **29**(9): p. 909-948.
58. Anastasiadis, S.H., et al., *Chain trapping in diblock copolymers near the ordering transition*. EPL (Europhysics Letters), 2000. **51**(1): p. 68.
59. Boudenne, N., et al., *Thermodynamic Effects on Internal Relaxation in Diblock Copolymers*. Physical Review Letters, 1996. **77**(3): p. 506-509.
60. Chrissopoulou, K., et al., *Dynamics of the Most Probable Composition Fluctuations of "Real" Diblock Copolymers near the Ordering Transition*. Macromolecules, 2001. **34**(7): p. 2156-2171.
61. Fytas, G., S.H. Anastasiadis, and A.N. Semenov, *Diffusive relaxation mode in diblock copolymer melts*. Macromolecular Symposia, 1994. **79**(1): p. 117-124.
62. Jian, T., et al., *Dynamics of Composition Fluctuations in Diblock Copolymer Solutions Far from and Near to the Ordering Transition*. Macromolecules, 1994. **27**(17): p. 4762-4773.
63. Patel, A.J., et al., *Relationship between structural and stress relaxation in a block-copolymer melt*. Physical Review Letters, 2006. **96**(25).
64. Patel, A.J., et al., *Dynamic Signatures of Microphase Separation in a Block Copolymer Melt Determined by X-ray Photon Correlation Spectroscopy and Rheology*. Macromolecules, 2010. **43**(3): p. 1515-1523.
65. Sanz, A., et al., *Relaxation processes in a lower disorder order transition diblock copolymer*. The Journal of Chemical Physics, 2015. **142**(6): p. 064904.
66. Ruegg, M.L., et al., *Condensed Exponential Correlation Functions in Multicomponent Polymer Blends Measured by X-ray Photon Correlation Spectroscopy*. Macromolecules, 2006. **39**(25): p. 8822-8831.
67. Hyun Jung, K., et al., *Synchrotron radiation studies of the dynamics of polymer films*. Journal of Physics: Condensed Matter, 2004. **16**(33): p. S3491.
68. Jiang, Z., et al., *Evidence for Viscoelastic Effects in Surface Capillary Waves of Molten Polymer Films*. Physical Review Letters, 2007. **98**(22): p. 227801.
69. Evans, C.M., et al., *Modulus, Confinement, and Temperature Effects on Surface Capillary Wave Dynamics in Bilayer Polymer Films Near the Glass Transition*. Physical Review Letters, 2012. **109**(3): p. 038302.
70. Jiang, Z., et al., *Entanglement Effects in Capillary Waves on Liquid Polymer Films*. Physical Review Letters, 2008. **101**(24): p. 246104.
71. Wang, S.-f., et al., *Anomalous Surface Relaxations of Branched-Polymer Melts*. Physical Review Letters, 2013. **111**(6): p. 068303.
72. Orsi, D., et al., *2D dynamical arrest transition in a mixed nanoparticle-phospholipid layer studied in real and momentum spaces*. Scientific Reports, 2015. **5**: p. 17930.
73. Koga, T., et al., *Reduced Viscosity of the Free Surface in Entangled Polymer Melt Films*. Physical Review Letters, 2010. **104**(6): p. 066101.
74. Hu, X., et al., *Observation of a low-viscosity interface between immiscible polymer layers*. Physical Review E, 2006. **74**(1): p. 010602.
75. Alvine, K.J., et al., *Capillary Wave Dynamics of Thin Polymer Films over Submerged Nanostructures*. Physical Review Letters, 2012. **109**(20): p. 207801.
76. Sinha, S.K., Z. Jiang, and L.B. Lurio, *X-ray Photon Correlation Spectroscopy Studies of Surfaces and Thin Films*. Advanced Materials, 2014. **26**(46): p. 7764-7785.

- 77. Westermeier, F., et al., *Connecting structure, dynamics and viscosity in sheared soft colloidal liquids: a medley of anisotropic fluctuations*. Soft Matter, 2016. **12**(1): p. 171-180.
- 78. Thurn-Albrecht, T., et al., *Photon correlation spectroscopy with high-energy coherent x rays*. Physical Review E, 2003. **68**(3): p. 031407.
- 79. Borland, M., *Progress Toward an Ultimate Storage Ring Light Source*. Journal of Physics: Conference Series, 2013. **425**(4): p. 042016.
- 80. Shinohara, Y., et al., *X-ray irradiation induces local rearrangement of silica particles in swollen rubber*. Journal of Synchrotron Radiation, 2015. **22**(1): p. 119-123.
- 81. Carnis, J., et al., *Demonstration of Feasibility of X-Ray Free Electron Laser Studies of Dynamics of Nanoparticles in Entangled Polymer Melts*. Scientific Reports, 2014. **4**.
- 82. Barty, A., et al., *Ultrafast single-shot diffraction imaging of nanoscale dynamics*. Nat Photon, 2008. **2**(7): p. 415-419.